J|A|C|S COMMUNICATIONS

Published on Web 11/29/2010

Highly Concentrated Graphene Solutions via Polymer Enhanced Solvent Exfoliation and Iterative Solvent Exchange

Yu Teng Liang and Mark C. Hersam*

Northwestern University, Department of Materials Science and Engineering and Department of Chemistry, 2220 Campus Drive, Evanston, Illinois 60208-3108, United States

Received August 24, 2010; E-mail: m-hersam@northwestern.edu

Abstract: Efficient graphene exfoliation in a nontraditional solvent, ethanol, is achieved through the addition of a stabilizing polymer, ethyl cellulose. Iterative solvent exchange is further demonstrated as a rapid, room-temperature, ultracentrifugation-free approach to concentrate the graphene solution to a level exceeding 1 mg/mL. The outstanding processability and electrical properties of these graphene inks are verified through the realization of aligned graphene−polymer nanocomposites and transparent conductive graphene thin films.

Graphene, a two-dimensional sp^2 hybridized lattice of carbon atoms, has generated intense interest due to its unique electronic,[1] mechanical,[2] chemical,[3] and catalytic properties.[4] Recent synthetic efforts have focused on the development of high-yield and scalable methods of generating graphene. These techniques include the direct exfoliation of either chemically modified or pristine graphene directly into various solvents.[4−7] For example, graphene oxide (GO) can be exfoliated from graphite via acidic treatments. The resulting GO flakes contain hydroxyl, epoxyl, carbonyl, and carboxyl groups along the basal plane and edges that render GO strongly hydrophilic.[8] The ease of dispersing GO in solution has facilitated the preparation of GO thin films and GO−polymer nanocomposites with interesting and potentially useful mechanical properties.[9,10] However, due to the defects and consequent disruption of the graphene band structure introduced during oxidation, GO is a poor electrical conductor. Although the level of oxygenation can be partially reversed through additional chemical reduction steps, significant quantities of structural and chemical defects remain.[11−14] Moreover, the electrical conductivity of reduced GO flakes lag behind their pristine counterparts.[13]

In an effort to circumvent the limitations of GO, recent efforts have focused on direct solution-phase exfoliation of pristine graphene.[15] Graphene sheets can be extracted using superacids[7] and through sonication in surfactant solutions[5,6] and organic solvents.[16−18] For example, superacids have demonstrated an unprecedented graphene solubility of 2 mg/mL through the protonation and debundling of graphitic sheets.[7] However, these solutions are not ideally suited for additional processing due to their acidity-dependent solubility and high reactivity. Direct exfoliation of graphene in surfactant solutions and select organic solvents has also been demonstrated with concentrations up to 0.3 mg/mL[6] and 1.2 mg/mL,[18] respectively, but these concentrations are achieved only following prolonged sonication times approaching 3 weeks in duration or extended ultracentrifugation.[5] These processing complexities represent a bottleneck for fundamental studies and applications that require well-dispersed, highly concentrated, pristine graphene solutions.

Herein, we demonstrate an alternative strategy for enhancing graphene exfoliation using a polymer−organic solvent solution. In addition, we present a room-temperature, ultracentrifuge-free concentration technique to generate graphene concentrations in excess of 1 mg/mL in organic solvents that otherwise yield poor graphene dispersibility. The resulting graphene inks are amenable to further processing, including casting into aligned graphene−polymer nanocomposites and blade coating to form thin films, as a result of their low solvent boiling point and noncausticity. Since this approach avoids oxidative conditions, the graphene maintains its superlative electronic properties, which can be exploited in applications that require highly conductive, mechanically flexible, and solution-processable coatings.

Due to the large mismatch between the surface energies of ethanol and graphite, ethanol is a relatively poor solvent for graphene exfoliation, yielding a postsedimentation concentration of 1.6 μg/mL.[16] To overcome this limitation, we utilize ethyl cellulose (EC) to enhance the ability of ethanol to exfoliate and suspend graphene flakes. A solution of 50 mg/mL natural graphite flakes in 1% w/v EC−ethanol was sonicated for 3 h and centrifuged at 7500 rpm for 4.5 h to remove the fast sedimenting graphite flakes. The resulting supernatant consists primarily of few-layer graphene sheets. Optical absorbance was taken to determine the graphene concentration using an absorption coefficient of 2460 L/g·m at 660 nm.[16] The addition of 1% EC significantly enhanced the graphene exfoliation efficiency by providing steric stabilization of the exfoliated flakes, yielding a postsedimentation concentration of 122.2 μg/mL. Despite this improvement, still higher concentrations are required to generate graphene inks that can be easily deposited and patterned.

Toward this end, we exploited iterative solvent exchange as a rapid room-temperature process to concentrate graphene solutions without the application of centrifugal force. In particular, a 1:5 volume ratio solution of terpineol and sedimented graphene solution was prepared and mixed to yield a solution with an initial graphene concentration of $C_0 = 102.4$ μg/mL. Water, four times the volume of this initial solution, was then added to form a hydrophilic ethanol solution. Owing to the hydrophobicity of the EC-stabilized flakes, graphene preferentially concentrates into the terpineol band on top of the ethanol−water solution (Figure 1A). This terpineol phase was then harvested, and additional sedimented graphene solution was added for the next concentration iteration. Concentration factors, C/C_0, were determined after each step through optical absorbance for three concentration iterations (Figure 1B). As expected, the concentration factors correspond roughly to the volumetric reduction of the graphene solution, producing a highly concentrated graphene ink at 1.02 mg/mL after three iterations. Additional iterations of solvent exchange yielded diminishing returns as the viscosity of the graphene ink began to interfere with material separation within the system. In order to verify the absence of flake agglomeration during the concentration

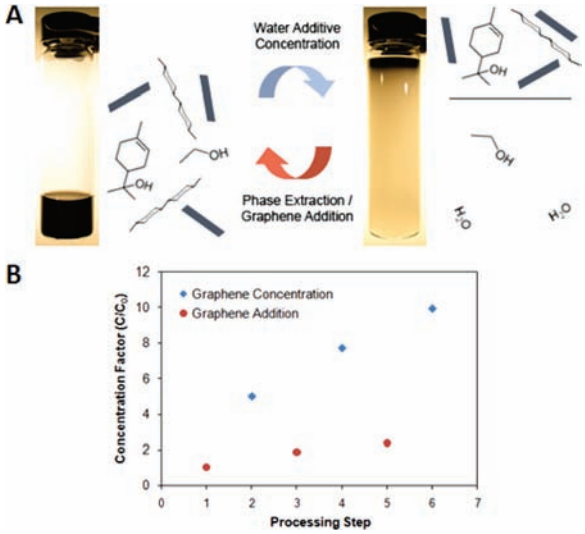

Figure 1. (A) Vials of a 1:5 mixture of terpineol and ethyl cellulose stabilized graphene−ethanol solution before and after water addition. Upon the addition of water, the hydrophobic graphene flakes preferentially separate into the concentrated terpineol fraction, leaving behind a predominantly ethanol and water mixture. (B) The concentration factor of graphene (C_0 = 102.4 μg/mL) is plotted after each solvent exchange concentration and graphene−ethanol addition step for three iterations.

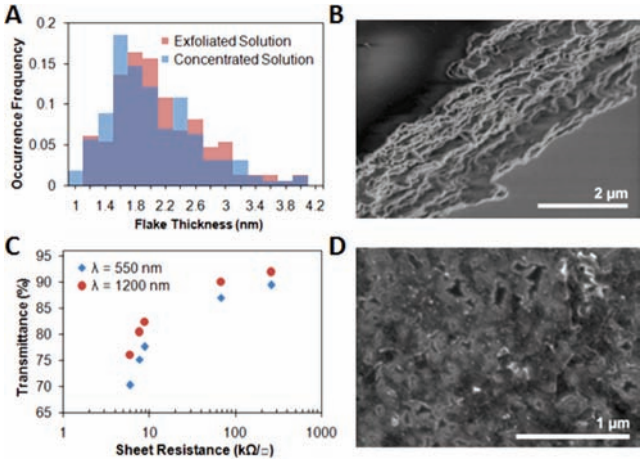

Figure 2. (A) Histograms of flake thickness for the initially exfoliated and third-iteration concentrated graphene solutions. (B) Scanning electron micrograph (SEM) of a graphene−ethyl cellulose nanocomposite fracture surface. (C) Optical transmittance versus sheet resistance for annealed transparent conductive thin films blade coated from the concentrated graphene inks. (D) SEM of an annealed graphene thin film.

process, atomic force microscopy was performed on over 140 flakes deposited from the sedimented graphene solution and the third iteration graphene ink (see Supporting Information). Both solutions exhibited similar flake thickness histograms peaked at approximately 1.6−1.8 nm (Figure 2A), suggesting minimal graphene agglomeration during the concentration process.

Graphene−polymer nanocomposites were solution cast from these graphene inks. The height reduction associated with anisotropic volume contraction during solvent evaporation resulted in the directional alignment of the graphene flakes within the nanocomposite. In Figure 2B, this alignment is evident on the fracture surface in the form of sheared terraces orthogonal to the direction of the volumetric contraction (see Supporting Information for a comparative image of the pure polymer fracture surface). The lack of protruding graphene flakes on the fracture surface not only is indicative of flake alignment but also suggests strong interactions between the polymer and graphene.

The electrical properties of thin films derived from the concentrated graphene ink were assessed via transparent conductor measurements. Due to their enhanced rheology, film forming capability, and dispersion stability, EC-stabilized graphene inks are amenable to blade coating onto a broad range of substrates. For example, graphene inks were blade coated onto glass slides at varying thicknesses, annealed at 400 °C for 30 min in air, and rinsed with acetone to produce transparent conductive thin films. Four point probe measurements of the film sheet resistance indicate that their electrical performances compare favorably to films deposited by vacuum filtration from sedimented surfactant graphene solutions (Figure 2C).[5] Electron microscopy performed on these conductive graphene thin films (Figure 2D) reveals a disordered network of graphene flakes with lateral dimensions ranging from approximately 50 to 400 nm. Raman spectra (see Supporting Information) provide further evidence that these graphene thin films possess low defect densities and negligible oxidation.

In conclusion, we have demonstrated that efficient graphene exfoliation can be achieved in ethanol through polymeric stabilization using ethyl cellulose. The resulting graphene solutions can be concentrated via rapid, room-temperature, ultracentrifugation-free iterative solvent exchange, ultimately yielding stable graphene inks at the 1 mg/mL level. The outstanding processability and electrical properties of the resulting inks enable the straightforward production of functional graphene-based materials including highly anisotropic polymer nanocomposites and transparent conductive thin films. Overall, this work is likely to impact ongoing efforts to understand and exploit solution-processable pristine graphene for fundamental studies and device applications.

Acknowledgment. This work was supported by the Department of Energy Institute for Catalysis in Energy Processes (DE-FG02-03ER15457) and a National Science Foundation Graduate Research Fellowship (Y.T.L.). SEM was performed in the NUANCE facility at Northwestern University, which is supported by the NSF-NSEC, NSF-MRSEC, Keck Foundation, and State of Illinois. Raman spectroscopy was performed at the Center for Nanoscale Materials at Argonne National Laboratory, which is supported by the U.S. Department of Energy, Office of Science, Office of Basic Energy Sciences, under Contract No. DE-AC02-06CH11357. We thank Dr. Gosztola for assistance with Raman spectroscopy.

Supporting Information Available: Graphene solvent processing, atomic force microscopy, nanocomposite and thin film photographs, and thin film optical absorbance and Raman spectra, and scanning electron micrograph of ethyl cellulose fracture surface. This material is available free of charge via the Internet at http://pubs.acs.org.

References

(1) Bolotin, K. I.; Sikes, K. J.; Jiang, Z.; Klima, M.; Fudenberg, G.; Hone, J.; Kim, P.; Stormer, H. L. *Solid State Commun.* **2008**, *146*, 351–355.
(2) Lee, C.; Wei, X. D.; Kysar, J. W.; Hone, J. *Science* **2008**, *321*, 385–388.
(3) Novoselov, K. S.; Geim, A. K.; Morozov, S. V.; Jiang, D.; Zhang, Y.; Dubonos, S. V.; Girgorieva, I. V.; Firsov, A. A. *Science* **2004**, *306*, 666–669.
(4) Wang, X.; Zhi, L.; Müllen, K. *Nano Lett.* **2008**, *8*, 323–327.
(5) Green, A. A.; Hersam, M. C. *Nano Lett.* **2009**, *9*, 4031–4036.
(6) Lotya, M.; King, P. J.; Khan, U.; De, S.; Coleman, J. N. *ACS Nano* **2010**, *4*, 3155–3162.
(7) Behabtu, N.; Lomeda, J. R.; Green, M. J.; Higginbotham, A. L.; Sinitskii, A.; Kosynkin, D. V.; Tsentalovich, D.; Parra-Vasquez, A. N. G.; Schmidt, D.; Kesselman, E.; Cohen, Y.; Talmon, Y.; Tour, J. M.; Pasquali, M. *Nat. Nanotechnol.* **2010**, *5*, 406–411.
(8) Lerf, A.; He, H.; Foster, M.; Klinowski, J. *J. Phys. Chem. B* **1998**, *102*, 4477–4482.
(9) Tung, V. C.; Allen, M. J.; Yang, Y.; Kaner, R. B. *Nat. Nanotechnol.* **2009**, *4*, 25–29.

(10) Stankovich, S.; Dikin, D.; Dommett, G. H. B.; Kohlhass, K. M.; Zimney, E. J.; Stach, E. A.; Piner, R. D.; Nguyen, S. T.; Ruoff, R. S. *Nature* **2006**, *422*, 282–286.
(11) Williams, G.; Seger, B.; Kamat, P. V. *ACS Nano* **2008**, *2*, 1487–1491.
(12) Gomez-Navarro, C.; Meyer, J. C.; Sundaram, R. S.; Chuvilin, A.; Kurasch, S.; Burghard, M.; Kern, K.; Kaiser, U. *Nano Lett.* **2010**, *10*, 1144–1148.
(13) Gomez-Navarro, C.; Weitz, R. T.; Bittner, A. M.; Scolari, M.; Mews, A.; Burghard, M.; Kern, K. *Nano Lett.* **2007**, *7*, 3499–3503.
(14) Bagri, A.; Mattevi, C.; Acik, M.; Chabal, Y. J.; Chhowalla, M.; Shenoy, V. B. *Nat. Chem.* **2010**, *2*, 581–587.
(15) Green, A. A.; Hersam, M. C. *J. Phys. Chem. Lett.* **2010**, *1*, 544–549.
(16) Hernandez, Y.; Lotya, M.; Rickard, D.; Bergin, S. D.; Coleman, J. N. *Langmuir* **2010**, *26*, 3208–3213.
(17) Hamilton, C. E.; Lomeda, J. R.; Sun, Z.; Tour, J. M.; Barron, A. R. *Nano Lett.* **2009**, *9*, 3460–3462.
(18) Khan, U.; O'Neill, A.; Lotya, M.; De, S.; Coleman, J. N. *Small* **2010**, *6*, 864–871.

JA107661G